



Hypermethylation of miR-181b in monocytes is associated with coronary artery disease and promotes M1 polarized phenotype via PIAS1-KLF4 axis

Zhonghua Wang, Chunlei Li, Xinyong Sun, Zhuqin Li, Jia Li, Lanfeng Wang, Yanming Sun

Department of Cardiology, The First Affiliated Hospital of Harbin Medical University, Harbin, China

Contributions: (I) Conception and design: Z Wang, Y Sun; (II) Administrative support: None; (III) Provision of study materials or patients: C Li, X Sun, Y Sun; (IV) Collection and assembly of data: Z Wang, Z Li, J Li, L Wang; (V) Data analysis and interpretation: J Li, L Wang; (VI) Manuscript writing: All authors; (VII) Final approval of manuscript: All authors.

Correspondence to: Yanming Sun, Department of Cardiology, The First Affiliated Hospital of Harbin Medical University, 23 Youzheng Street, Nangang District, Harbin 150001, China. Email: yanmingsun2019@163.com.

Background: Dysregulated microRNAs are involved in the macrophage polarization and atherosclerotic development. Apart from microRNAs, alteration in DNA methylation is considered as one of the most frequent epigenetic changes. The purpose of the research is to investigate the altered methylation status of miR-181b in the circulating monocytes from patients with coronary artery disease (CAD) and explore the underlying mechanisms.

Methods: We examined the methylation status of miR-181b in purified circulating monocytes from patients with CAD and healthy controls. We then transfected monocytes with miR-181b mimics and determined the role of miR-181b on the phenotypic switch of macrophages and inflammatory response. DNA methylation levels determined by MethyLight PCR and pyrosequencing at the promoter of miR-181b significantly increased in CAD patients. Based on TargetScan database, we identified PIAS1 as the target gene of miR-181b and explored the interaction of miR-181b and PIAS1 by Dual-Luciferase assay, quantitative PCR and immunoblots. We also investigated the role of miR-181b and PIAS1 on macrophage polarization and inflammation.

Results: Hypermethylation at the promoter of miR-181b directly contributed to the decrease of miR-181b activity and expression. Overexpression of miR-181b reduced M1 polarization and facilitated M2 polarization determined by quantitative PCR. While knockdown of PIAS1 induced KLF4 degradation and SUMOylation in monocytes, miR-181b mimics reverse the KLF4 SUMOylation via suppression of PIAS1. Moreover, KLF4 SUMOylation by PIAS1 reversed M1 polarization induced by depletion of miR-181b in monocytes.

Conclusions: Hypermethylation of miR-181b induces M1 polarization and promotes atherosclerosis through activation of PIAS1 and KLF4 SUMOylation in macrophages.

Keywords: Coronary artery disease (CAD); miR-181b; PIAS1; KLF4 SUMOylation; macrophage polarization

Submitted Apr 01, 2020. Accepted for publication Jun 18, 2020.

doi: 10.21037/cdt-20-407

View this article at: <http://dx.doi.org/10.21037/cdt-20-407>

Introduction

Arteriosclerotic cardiovascular disease (ASCVD) is the leading cause of morbidity and mortality worldwide (1). Atherosclerosis is considered as a chronic inflammatory

and multifactorial disease. Endothelial activation and recruitment, vascular smooth muscle cell (VSMC) proliferation and migration, monocyte infiltration, macrophage polarization and foam cell formation are

involved in atherogenesis. In this respect, macrophage played pivotal roles in all stages of atherosclerosis, from lesion initiation, expansion and rupture (2). Apart from a minority of macrophage-like cells derived from smooth muscle cells, resident macrophages in plaques are primarily from circulating monocytes (3). Furthermore, resident macrophages switch to different phenotypes in response to diverse environments and intracellular signaling pathways during the different phases of atherosclerosis (4). The different phenotypes of macrophages allow them to evolve to homeostatic imbalance in intracellular lipids, metabolites and inflammatory response. In this regard, activated macrophages are capable of polarizing towards a classical phenotype M1 induced by interferon- γ (IFN- γ) and the broad-spectrum Toll-like receptor (TLR) ligand lipopolysaccharide (LPS). An alternative phenotype M2 is induced by T helper 2 (Th2) cytokines interleukin-4 (IL-4) (5,6). Recent researches propose a series combination of markers to ascertain and characterize macrophage polarization (7,8). There is also extensive evidence suggesting that depletion of KLF4 in macrophages and vascular smooth muscle cells (VSMCs) resulted in remarkable reductions in plaque burden and increases in plaque stability (9). In addition, modulation of macrophage and VSMC phenotype switch and inflammation via KLF4 plays a critical role in atherogenesis (10,11).

MiRNAs are considered as small non-coding RNAs that play an important role in the post-transcriptional regulation of gene expression by blocking mRNA translation or inducing mRNA degradation. Accumulating epidemiological trials and experimental studies have demonstrated that miRNAs are involved in the development of atherosclerosis (12-14). More specifically, RNA sequencing followed with quantitative RT-PCR has obtained differentiated miRNA expression profiles between M1 and M2 polarization and determined the involvement of miR-181b, miR-34a, miR-223 and miR-125b in macrophage activation and polarization (12). DNA methylation, another important epigenetic pattern, occurs when methyl groups are added to cytosines by DNA methyltransferases (DNMTs). The methylated cytosines primarily reside in CpG islands around transcription start sites and mitigate gene transcription by blocking binding sites for transcription factors. Growing bodies of evidence suggest that aberrant DNA methylation in specific cell types emerge as promising biomarkers for cardiovascular diseases (15). Likewise, DNA methylation play causal roles in miRNA dysregulation and chronic inflammation in

macrophages (16). DNA methylation also participates in the initiation and progression of atherosclerosis (15). However, the crosstalk between DNA methylation and miRNAs driving macrophage polarization and atherogenesis remains poorly understood.

In this study, we sought to explore the expression levels and methylation levels of candidate miRNAs in monocytes from healthy controls and patients with coronary artery disease (CAD). Furthermore, we determined the methylation status of candidate miRNA during macrophage polarization. Cellular and molecular experiments were also performed to explore the mechanism underlying candidate miRNA and macrophage polarization.

Methods

Study population

The clinical trial was approved by the First Affiliated Hospital of Harbin Medical University Ethics Committee (Ethical approval ID: HMU-2018-124). The informed written consent was provided in accordance with the Declaration of Helsinki (as revised in 2013) and obtained from the whole enrollment.

A total of 150 patients who were suspicious with presentations and symptoms related to CAD received angiography as routine diagnostic procedure. Patients who were complicated with congenital heart disease, cardiomyopathy, autoimmune diseases, acute infections, chronic obstructive pulmonary disease (COPD), tuberculosis, severe kidney or liver diseases, and cancers were excluded from the study.

Quantification of coronary plaques

At least six projections of left and right coronary artery were obtained using coronary angiography in each individual. The segments of coronary plaques were assessed according to the 18-segment SCAI classification (17). In brief, significant CAD was defined as the presence of luminal diameter narrowing $\geq 50\%$ in the left anterior descending artery, left circumflex artery, right coronary artery and their main branches. Left main trunk stenosis was considered as two-vessel disease. The burdens of atherosclerotic plaques were evaluated by the length of plaque (>20 mm as long lesions), the degree of stenosis with and without calcification, and the number of coronary vessels with significant stenosis. The experts recorded the highest

degree of stenosis in CAD patients with multivessel diseases for further investigation.

Monocyte isolation and purification

Leukocyte subsets separation and purification were performed immediately after the blood draw as previously described with minor modification (18). Briefly, peripheral blood mononuclear cells (PBMCs) and granulocytes were separated using density centrifugation on Ficoll-Paque (Sigma, USA), followed by centrifugation at 350 g for 20 minutes. Monocytes were purified from PBMCs by positive selection using anti-CD14 antibodies conjugated paramagnetic microbeads (Miltenyi Biotec, Germany), then the cells were separated according to standard protocols for magnetic-activated cell sorting (MACS) using LS columns and MidiMACS separator (Miltenyi Biotec, Germany). A separate sample of 1×10^5 monocytes was taken from individual for purity validation by flow cytometer (BD Biosciences, USA).

MiRNA mimics and inhibitor transfection

MiR-181b mimics, miR-181b inhibitors (anti181b), small interfering against PIAS1 (siPIAS) and the corresponding negative control (NC) were purchased from Genepharma Incorporation (Genepharma, China). The purified cells were transfected with miR-181b mimics, miR-181b inhibitors, siPIAS1 or their corresponding NC using Hiperfect transfection reagent (Qiagen Incorporation, Germany) based on the manufacturer's instructions.

Induction of macrophage polarization

Following apheresis, circulating monocytes were plated (24 well plates, 3×10^5 cells per well), allowed to adhere for 24 hours, washed with culture solutions and cultured in 20% FBS/RPMI with recombinant M-CSF at a concentration of 100 ng/mL (Peprotech Incorporation, USA) for 4 days (M0 phenotype). Macrophages were washed and treated for 12 hours with RPMI +5% FBS alone, LPS at a concentration of 100 ng/mL and recombinant interferon gamma (IFN- γ , Peprotech Incorporation, USA) at a concentration of 20 ng/mL for differentiation to the M1 phenotype, or recombinant IL-4 at a concentration of 20 ng/mL (Peprotech Incorporation, USA) for differentiation to the M2 phenotype. To determine whether STAT1 mediated the role of miR-181b

in macrophage polarization, macrophages were pretreated with 50 μ M of Fludarabine (Selleck, USA) for 12 hours.

DNA extraction, bisulfite conversion and MethyLight PCR

Briefly, the genomic DNA was isolated by using DNeasy blood and tissue kit (Qiagen, Germany). All unmethylated cytosines in genomic DNA were converted to uracil by sodium bisulfite conversion (EpiTect kit, Qiagen, Germany), while the methylated cytosines were protected. MethyLight PCR was used to determine DNA methylation at the promoter of miR-181b as previously described (19). The percentage methylated of reference (PMR) value was calculated. CpGenome Universal Methylated DNA (Thermo Fisher, USA) served as a positive control. The exact methylation levels of miR-181b measured by methylated PCR were presented by PMR value relative to the positive control as described previously (19). The primers designed for MethyLight PCR are listed in *Table S1*.

Pyrosequencing quantitative methylation analysis

From selected CpG island, a DNA fragment containing 4 CpG dinucleotides was PCR-amplified (*Table S1*). The PCR products were subjected to pyrosequencing on PyroMark Q24 (QIAGEN, Valencia, CA, USA). We calculated the methylation index of each CpG dinucleotide by the PyroMark Q24 analysis software.

Dual luciferase reporter assay

HEK293T cells were cultured in DMEM (Gibco, USA) containing 10% FBS (Gibco, USA), 1% penicillin and streptomycin. PIAS1 3'UTR was cloned into the dual-luciferase reporter plasmid psiCHECK-2 (Promega, USA). Constructs carrying the fragment of the mutated PIAS1 3' untranslated coding regions (UTR) without the putative miR-181b binding sequence served as the mutated control. HEK293T cells were co-transfected with psiCHECK-PIAS1-3'UTR (Luci-PIAS1-WT) or with psiCHECK-PIAS1-3'UTR mutant (Luci-PIAS1-Mut), and miR-181b mimics using Lipofectamine 2000 for 24 hours. Furthermore, pGL4.45 (luc2P/ISRE/Hygro) plasmid was purchased from Promega corporation (Promega, USA) and was used to determine the transcription activity of STAT1 responsive elements.

Specific primers containing KpnI restriction site (Mir-181b-LUC-KpnI) were designed according to the sequence

(from -1,316 to -1,183 bp relative to transcription start site) of human miR-181b promoter (*Table S1*). The amplified fragments were digested with KpnI restriction enzyme and inserted into pGL3-basic vector (Promega, USA). The promoter constructs were sequenced and incubated overnight with three units of CpG methyltransferase in the presence of 1 mmol/L S-adenosylmethionine according to the manufacturer's recommendation (New England Biolabs, UK). Then 1 µg of pGL3-basic (containing methylated or unmethylated miR-181b fragments) and 100 ng of Renilla plasmid (Promega, USA) were co-transfected into HEK293T using Lipofectamine 2000 for 24 hours. Luciferase and Renilla signals were measured 48 hours after transfection using Dual-Luciferase reporter assay kit (Promega, USA). The luciferase activity was normalized against Renilla activity. The experiments were performed in triplicate for each construct.

RNA isolation and quantitative RT-PCR

The isolation and purification of total RNA and quantitative RT-PCR was performed as previously described (20). Comparative cycle threshold (Ct) method was used to calculate expression of the miR-181b and the expression of U6 small nuclear RNA was considered as reference. The primer sequences predesigned for quantitative RT-PCR are tabulated in *Table S1*.

Western blots

The proteins from tissues and cells were obtained using a Cell Lysis extraction kit (Beyotime Biotechnology, Shanghai, China). The concentrations of the proteins were determined by using the BCA protein assay (Beyotime Biotechnology, China). Equal amounts (10 µg) of protein were constantly separated by proper concentrations of SDS-PAGE and transferred onto polyvinylidene difluoride membranes (PVDF, Millipore, USA). After blocked with 5% nonfat milk, PVDF membranes were incubated with the appropriate primary antibodies against P1AS1 (1:800; ab32219, Abcam, Cambridge, USA), KLF4 (1:1,000; ab215036, Abcam, Cambridge, USA), KLF6 (1:500; sc-134374, Santa Cruz, USA), YAP (1:500; sc-101199, Santa Cruz, USA), Fra-1 (1:500; sc-48424, Santa Cruz, USA) and GAPDH (1:2,000; 2118, Cell Signaling Technology, USA) at 4 °C for 16 hours. Then the membranes were incubated with horseradish peroxidase-conjugated

secondary antibodies (1:2,500; catalog 7072, Cell Signaling Technology, USA) at room temperature for 2 hours. The bands were finally detected with ECL Detection Reagents (Thermo Fisher, USA).

Co-immunoprecipitation

The cells were lysed using a Cell Lysis extraction kit (Beyotime Biotechnology, Shanghai, China). After purification, the supernatants were obtained and incubated with the KLF4 antibody (1:100; ab215036, Abcam, Cambridge, USA) at 4 °C overnight. The immunoprecipitation was recovered by combination to protein A/G beads (Santa Cruz, USA) for 3 hours at 4 °C. After washing in lysing buffer, the immunoprecipitants were detected by immunoblot analysis.

Immunofluorescence staining

Macrophages transfected with miR-181b mimics and scramble mimics for 48 hours. The prepared cells were fixed with 3.6% paraformaldehyde for 10 minutes, permeabilized with 0.2% Triton X diluted in PBS (PBST), and subsequently blocked by treatment of cells with 3% bovine serum albumin (Beyotime Biotechnology, Shanghai, China). Then the cells were incubated with 5% normal goat serum diluted in PBST for 20 minutes at room temperature. CD206 antibodies (diluted 1:50, BeckmanCoulter, USA) were added and incubated at 4 °C for 16 hours and then the cells were labeled with goat-anti-mouse secondary antibodies coupled to cyanine 3 (Beyotime Biotechnology, Shanghai, China) at room temperature for 1 hour. Following appropriate washing steps with PBS and distilled water, nuclei were counterstained with DAPI (Beyotime Biotechnology, Shanghai, China).

Statistic analysis

Statistical analyses were performed with SPSS software (version 17.0, IBM, USA). The data were presented as mean ± standard deviation (SD). Differences between two group was analyzed with Student's *t*-test. Differences between multiple groups were initially compared using one-way ANOVA test and then, if appropriate, between-group post-hoc tests were analyzed with Bonferroni comparison. Differences were regarded as statistically significance for $P < 0.05$.

Table 1 Baseline characteristics of study population

Characteristics	Control (n=60)	CAD (n=90)	P value
Age, years	69.7±8.4	68.3±8.9	NS
Male, n (%)	20 (33.3)	52 (57.8)	0.003
Smoking, n (%)	14 (23.3)	21 (23.3)	NS
Diabetes, n (%)	7 (11.7)	10 (11.1)	NS
Fasting glucose, mmol/L	5.4±2.0	5.9±1.9	NS
Hypertension, n (%)	19 (31.7)	24 (26.7)	NS
TC, mmol/L	4.5±0.9	4.8±1.1	NS
TG, mmol/L	1.4±0.3	1.7±0.5	NS
LDL-C, mmol/L	2.6±0.9	2.8±1.0	NS
HDL-C, mmol/L	0.9±0.3	1.1±0.4	NS
BUN, mmol/L	5.7±1.2	5.9±1.8	NS
Creatinine, mg/L	75.8±18.4	79.5±21.5	NS
hs-CRP, mg/L	1.04±0.27	1.14±0.29	NS
cTnT, µg/L	0.01±0.01	0.02±0.01	NS
CK-MB, ng/mL	35.8±9.4	37.3±9.2	NS
Coronary angiography, n (%)			
Long lesions	–	21 (23.3)	
Culprit vessels, n (%)			
1-vessel	–	53 (58.9)	
2-vessel	–	28 (31.1)	
≥3-vessel	–	9 (10.0)	
Stenosis, n (%)			
Moderate	–	50 (55.6)	
Severe	–	37 (41.1)	
Occlusion	–	3 (3.3)	

BUN, blood urine nitrogen; CAD, coronary artery disease; HDL-C, high-density lipoprotein cholesterol; LDL-C, low-density lipoprotein cholesterol; TC, total cholesterol; TG, triglyceride.

Results

MiR-181b is hypermethylated in peripheral monocytes from CAD patients

The characteristics of enrolled population is shown in *Table 1*. The locations of miR-181b promoter and CpG sites are shown in *Figure 1A*. The methylation status of miR-181b in circulating CD14⁺ monocytes isolated from CAD patients was remarkably higher than that from control group (control PMR 12.37±8.28 vs. CAD PMR 20.46±8.42,

$P < 0.01$, *Figure 1B*). By contrast, the miR-181b expression levels were greatly reduced in CAD patients relative to control group (*Figure 1C*). To further investigate the effect of miR-181b methylation on plaque characteristics, we stratified CAD patients by lesion length, the figure of culprit vessels and atherosclerotic burden. Interestingly, we found a gradual increase in the miR-181b methylation as increase in the number of culprit vessels, lesion length and the degree of stenosis (*Figure 1D,E,F*).

To further understand the precise methylation

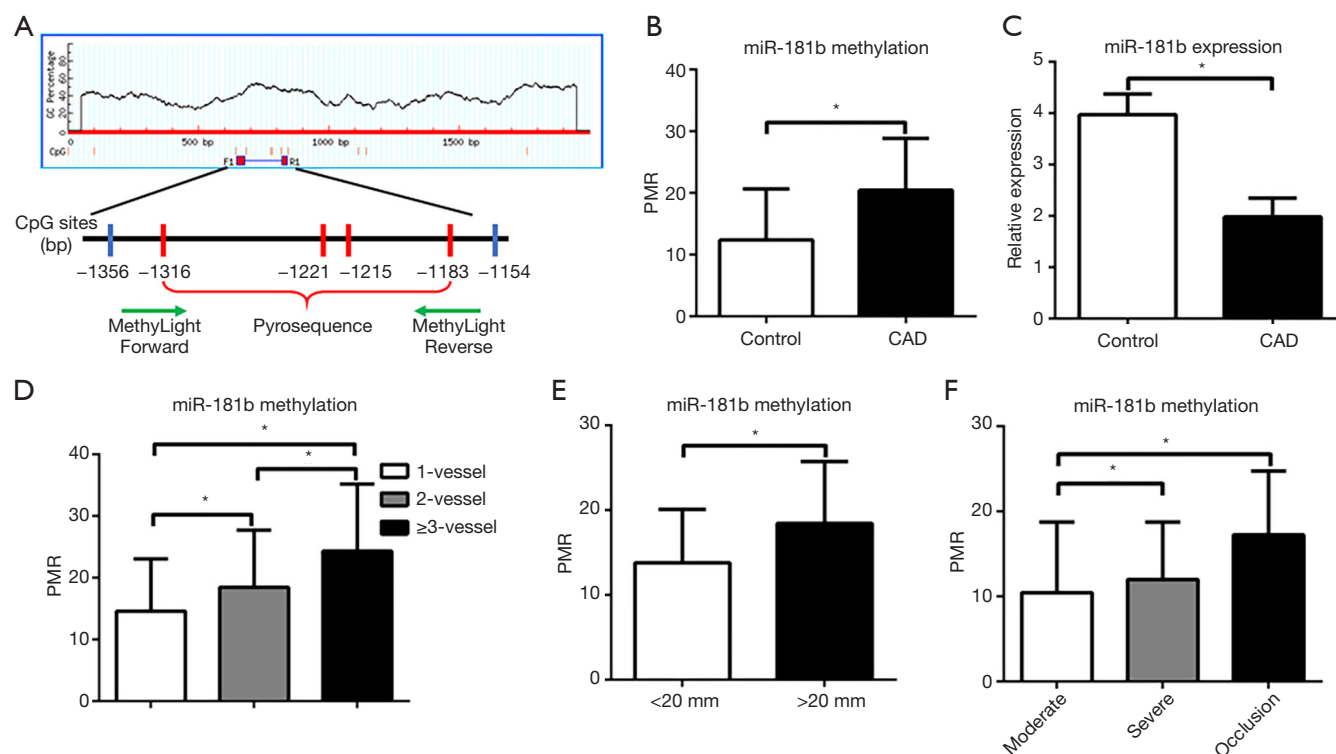


Figure 1 MiR-181b hypermethylation is associated with the incidence and severity of coronary artery disease. (A) Schematic diagram of miR-181b promoter. Upper, CG percentages within the target region (start from $-2,000$ bp relative to transcription start site) of miR-181b promoter. Bottom, red pillars show the CpG sites within the sequencing fragment of miR-181b promoter. Green arrow indicates the MethyLight PCR primer predesigned for miR-181b methylation. (B) Comparison of miR-181b methylation in circulating CD14⁺ monocytes between controls and patients with coronary artery disease (CAD). (C) Comparison of miR-181b expression in circulating CD14⁺ monocytes between controls and patients with CAD. (D) Comparison of miR-181b methylation in circulating CD14⁺ monocytes from CAD patients according to the number of culprit vessels. (E) Comparison of miR-181b methylation in circulating CD14⁺ monocytes from CAD patients according to the length of plaque detected by coronary angiography. (F) Comparison of miR-181b methylation in circulating CD14⁺ monocytes from CAD patients according to the degree of stenosis. Data are presented as mean \pm SD. *, $P < 0.05$. PMR, percentage methylated of reference.

percentages within the promoter of miR-181b at indicated CpG sites, we next conducted pyrosequencing in CD14⁺ monocytes from 20 healthy controls and 20 CAD patients respectively. On basis of pyrosequencing, we accentuated that individual methylation percentage of 4 candidate CpG sites and the average methylation percentage of all analyzed CpG sites in CAD patients were consistently higher in CAD patients than those in control group (Figure 2A,B). In order to verify the function of methylation of CpG sites on miR-181b expression, we showed that as compared to normal vectors, the methylated vectors inserted with the indicated fragments of miR-181b promoter significantly repressed the transcription activities by 42.3% in HEK293T cells, reflecting that alteration in methylation status of miR-181b

promoter is able to suppress miR-181b promoter activity and expression (Figure 2C).

Effect of miR-181b on macrophage polarization

We then sought to determine whether miR-181b affected macrophage polarization and activated inflammation. Result of quantitative RT-PCR showed that the expression levels of miR-181b were downregulated in macrophages induced by LPS and IFN- γ , while significant upregulation of miR-181b was observed in IL-4-treated macrophages (Figure 3A). To investigate the influence of miR-181b on macrophage polarization, we tested the expression of macrophage polarization markers by quantitative PCR.

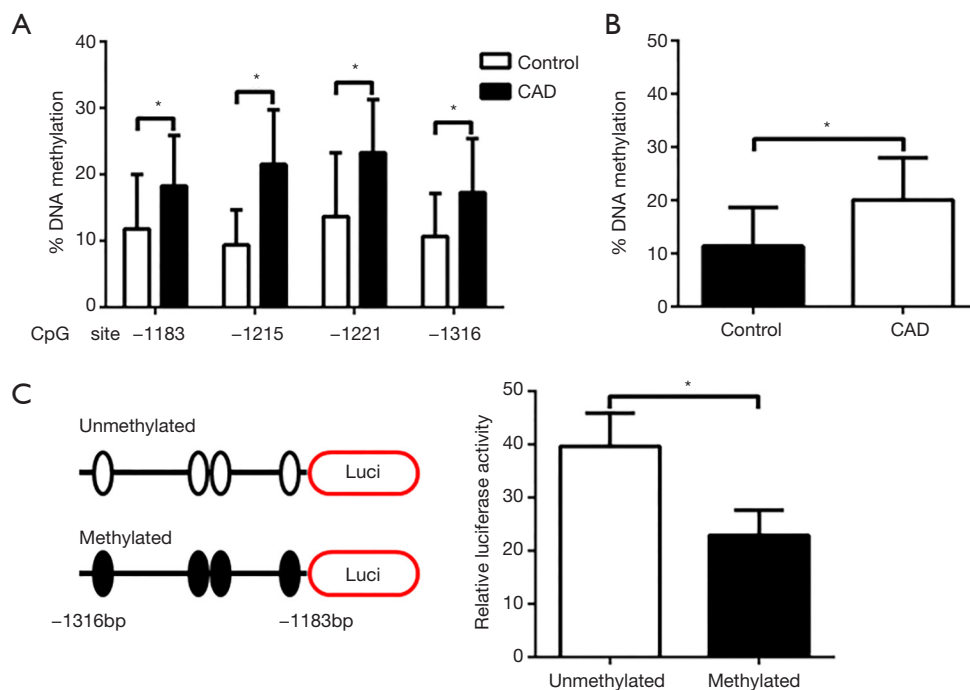


Figure 2 MiR-181b methylation impairs its expression. (A) Pyrosequencing to identify miR-181b methylation percentage at each CpG site in circulating CD14⁺ monocytes between controls (n=20) and patients with coronary artery disease (CAD) (n=20). (B) Quantification of average methylation percentages from all measured CpG sites by pyrosequencing in controls and patients with CAD. (C) Relative luciferase activity of pGL3-basic containing the fragment of unmethylated and methylated miR-181b promoter (mir-181b-LUC-KpnI). Relative luciferase activity is normalized with an internal pGL-TK Renilla activity. Each experiment was performed in triplicate. Data are presented as mean \pm SD. *, P<0.05.

Overexpression of miR-181b significantly suppressed the expression of M1 phenotype markers such as IL-6 and TNF- α in macrophages stimulated by LPS and IFN- γ , but enhanced the expression of M2 markers such as Arg1 and CD206 in IL-4-induced macrophages (Figure 3B,C,D,E). Immunofluorescence staining of macrophages transfected with scramble or miR-181b mimics exhibited that the density and distribution of M2 phenotype marker CD206 was significantly increased in miR-181b-upregulated group as compared with scramble mimics group, implying that miR-181b promotes macrophages to polarize into M2 subset (Figure 3F).

Effect of miR-181b on KLF4 expression and SUMOylation

To identify the potential molecular determinants involved in miR-181b-mediated macrophage polarization, we turned our attention to the effect of miR-181b on transcription factors priming macrophage polarization. Overexpression

of miR-181b resulted in remarkable increase in the protein expression of KLF4 (Figure 4A). In contrast to KLF4 upregulation, we could not detect any induction of other known transcription factors in macrophages transfected with miR-181b mimics (Figure 4B). In fact, we failed to detect prominent discrepancy in the mRNA expression of KLF4 in macrophages transfected with scramble and miR-181b mimics (Figure 4C). This seeming contradiction inspired us to explore the post-transcriptional mechanism regulating miR-181b-induced KLF4 alteration. We pretreated macrophage with MG132 (10 μ M), a potent proteasome inhibitor known to abrogate the levels of protein ubiquitylation and SUMOylation, finding that MG132 restored the reduced protein expression of KLF4 induced by miR-181b inhibition (Figure 4D). We then performed SUMOylation assay and observed an accumulation of SUMOylated KLF4 in macrophages transfected with anti181b, indicating that depletion of miR-181b augmented KLF4 SUMOylation and degradation (Figure 4E).

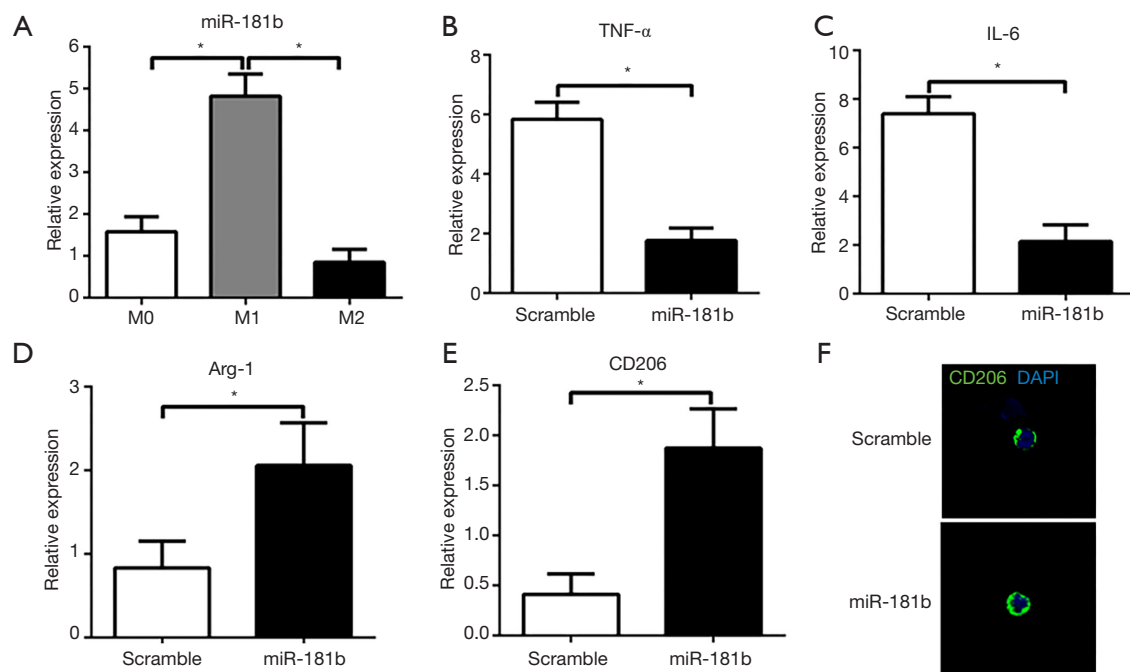


Figure 3 MiR-181b is essential for M1 polarized phenotype of macrophages. (A) MiR-181b is upregulated in M1 polarized phenotype of macrophages. (B,C,D,E) Quantification of M1 and M2 markers in macrophages transfected with scramble and miR-181b mimics. Macrophages are pretreated with LPS (100 ng/mL) and IFN- γ (20 ng/mL) for M1 polarization. Macrophages are pretreated with IL-4 (20 ng/mL) for M2 polarization. TNF- α and IL-6 are considered as M1 markers, while Arg-1 and CD206 are defined as M2 markers. (F) Representative immunofluorescence images of CD206 as M2 marker in macrophage transfected with scramble and miR-181b mimics. Each experiment was performed in triplicate. Data are presented as mean \pm SD. *, $P < 0.05$.

MiR-181b bound to PIAS1 and inhibited PIAS1 expression

To investigate the potential mechanisms involved in miR-181b-mediated KLF4 SUMOylation and M1 polarization, we searched for other putative target genes of miR-181b using online bioinformatic database, TargetScan Release 7.2 (www.targetscan.org). Among numerous conserved targets of miR-181b, PIAS1 was selected based on its role on protein degradation and SUMOylation. As shown in *Figure 5A*, there is a reserved binding sequence of miR-181b within the 3'UTR of PIAS1 mRNA. The binding fragment within the 3'UTR of PIAS1 was amplified and cloned into plasmid, followed with evaluation with Dual Luciferase Reporter Assay. The results showed that overexpression of miR-181b alleviated the luciferase activities of Luci-PIAS1-WT but did not alter the luciferase activities of Luci-PIAS1-Mut, suggesting that miR-181b was capable of directly binding to the 3'UTR of PIAS1 (*Figure 5B*). Furthermore, the results from quantitative PCR and immunoblots consistently

showed that the expression of PIAS1 was dramatically decreased after up-regulation of miR-181b (*Figure 5C,D*). Accordingly, the expression levels of PIAS1 were markedly higher in circulating monocytes from CAD patients than those from healthy controls (*Figure 5E*). According to the prior report, we elucidated the effect of PIAS1 on activated STAT1 using Dual Luciferase assay, indicating that knockdown of PIAS1, in the presence of IFN- γ , resulted in increased Luciferase activity of STAT1 responsive elements (*Figure 5F*) (21).

MiR-181b silencing induced KLF4 SUMOylation via PIAS1 activation

To further determine the relationship among miR-181b, PIAS1 and KLF4, the macrophages were co-transfected with miR-181b inhibitors and siPIAS1, followed by western blots, co-immunoprecipitation and quantitative PCR. Knockdown of miR-181b in macrophages enhanced PIAS1 and decreased the protein levels of KLF4, which

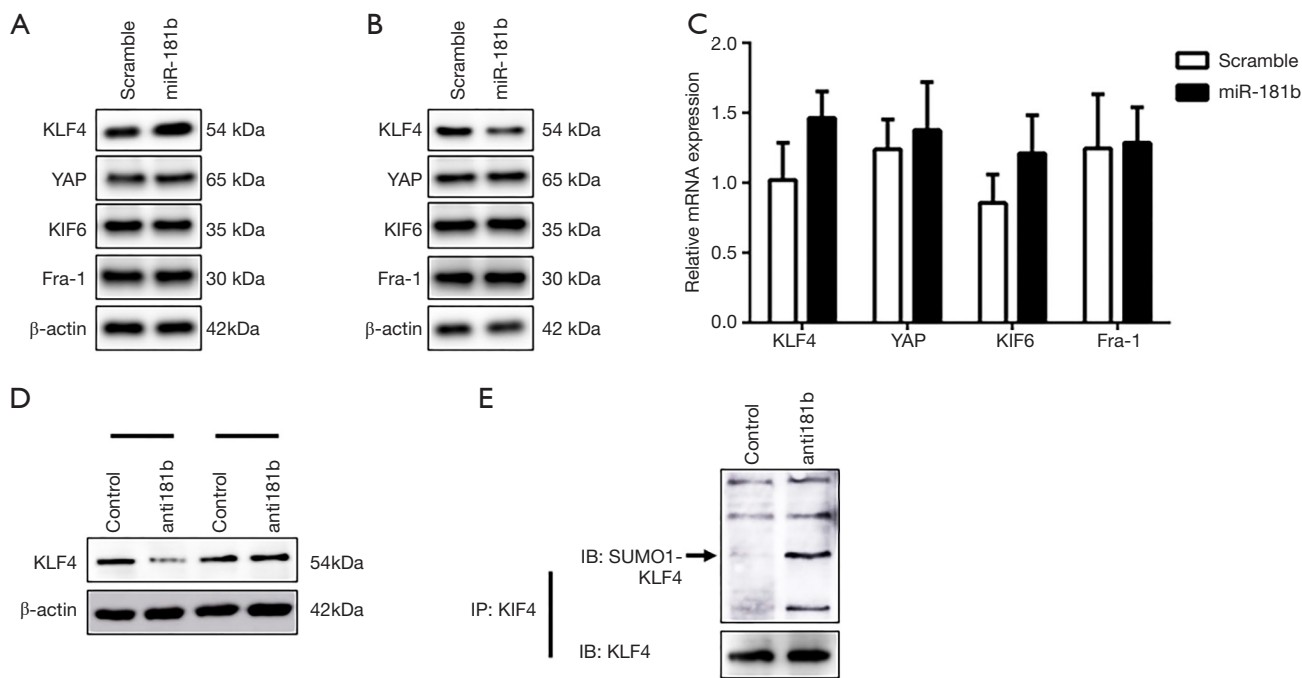


Figure 4 Inhibition of miR-181b drives KLF4 SUMOylation. (A) Western blots show that overexpression of miR-181b promotes the protein expression of KLF4. (B) Western blots show that knockdown of miR-181b suppresses the protein expression of KLF4. (C) Quantitative PCR shows that overexpression of miR-181b does not the mRNA expression of KLF4. (D) Proteasome inhibitor MG132 reverses the protein expression of KLF4 reduced by miR-181b inhibitors (anti181b). (E) Endogenous SUMO1 conjugates of KLF4 are determined by co-immunoprecipitation in the lysates of macrophages transfected with anti181b. Human macrophages from circulating monocytes were maintained in 20% FBS/RPMI with recombinant M-CSF (100 ng/mL). Each experiment was performed in triplicate. Data are presented as mean \pm SD.

were reversed by the downregulation of PIAS1 (Figure 6A). Consistent with the findings, knockdown of miR-181b in macrophages increased SUMO1-conjugated KLF4 SUMOylation with this effect being counteracted by knockdown of PIAS1 (Figure 6A). The results of quantitative PCR showed that depletion of PIAS1 could counteract the suppressive effects of miR-181b inhibitors on Arg1 and CD206 expression, whereas supplements with siPIAS1 inhibited the excessive TNF- α and IL-6 expression induced by miR-181b inhibitors (Figure 6B). We next sought to determine whether miR-181b facilitated M1 polarized phenotype via regulating STAT1 or KLF4. As shown in Figure 6C, transfection with KLF4 siRNA substantially reversed the downregulation of TNF- α and IL-6 stimulated by overexpression of miR-181b. Nevertheless, specific STAT1 inhibitor Fludarabine did not affect the expression of TNF- α and IL-6 in the presence of miR-181b mimics (Figure 6D). These data suggested

that miR-181b modulated macrophage polarization and abrogated KLF4 SUMOylation by interaction with PIAS1 (Figure 7).

Discussion

Recent studies have reported that miR-181b has critical function in numerous cancers, cardiac hypertrophy and kidney injury, but little is known about its roles in the progression of macrophage polarization (20,22-24). In this report, we underscore the predictive value of miR-181b hypermethylation in the incidence and development of CAD. Moreover, we provide a proof of principle for the genetic gain and loss of miR-181b regulating macrophage polarization via targeting PIAS1 and KLF4 SUMOylation.

The atherosclerotic microenvironmental milieu, which is composed of lipid metabolites, cytokines and non-coding RNAs secreted from parenchymal vascular cells

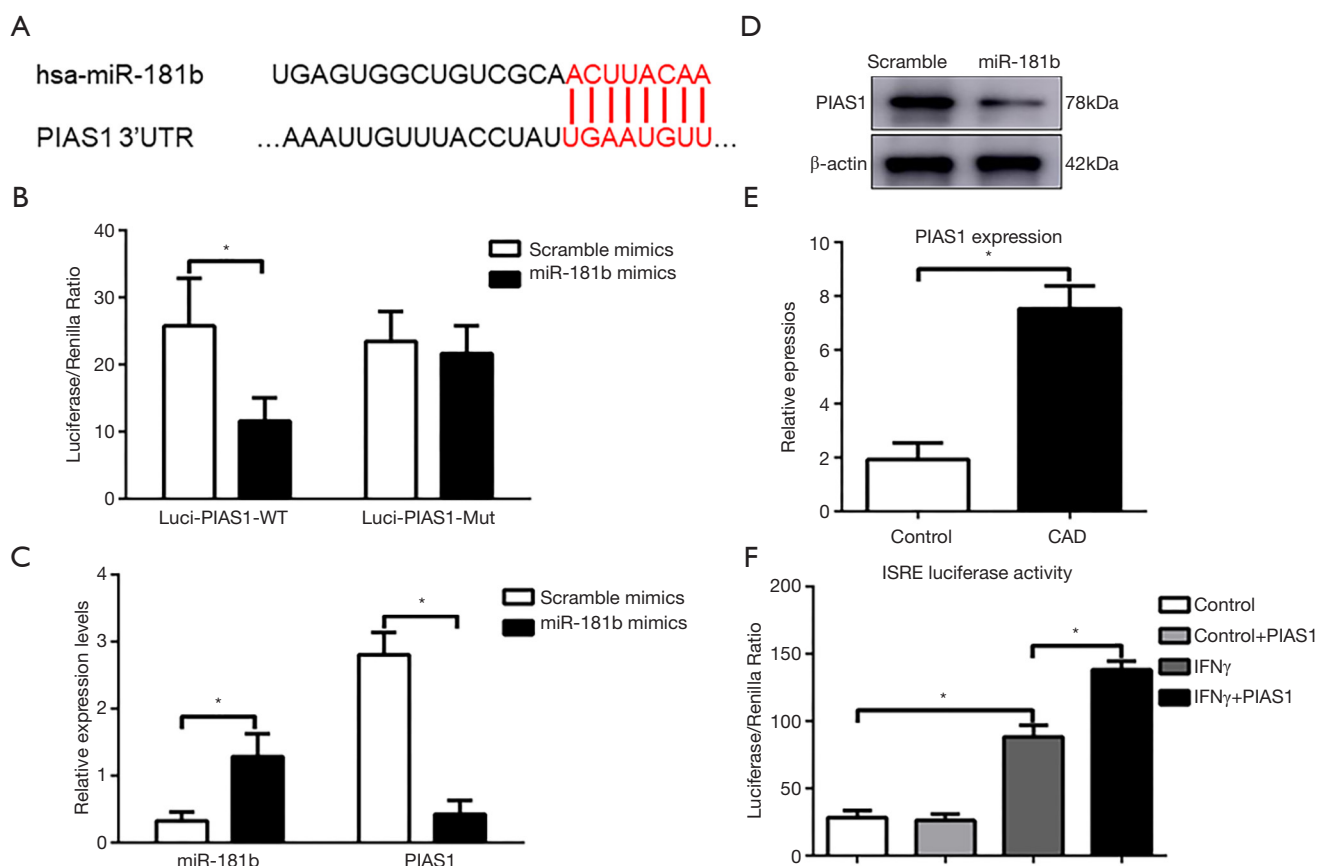


Figure 5 MiR-181b directly targets PIAS1. (A,B) Construction of Luciferase-wildtype UTR vectors (Luc-PIAS1-WT) and the corresponding luciferase-mutated UTR vectors (Luc-PIAS1-mutant). Transfection with miR-181b mimics significantly reduces luciferase activities, whereas it does not affect the luciferase activity in the mutant construct compared with scramble mimics transfection. (C) Quantitative PCR shows that overexpression of miR-181b results in the downregulation of PIAS1. (D) Western blots show that overexpression of miR-181b inhibits the protein expression of PIAS1 in macrophages. Human macrophages from circulating monocytes were maintained in 20% FBS/RPMI with recombinant M-CSF (100 ng/mL), followed by treatment with LPS (100 ng/mL) and IFN- γ (20 ng/mL) for M1 polarization. (E) Comparison of PIAS1 expression in circulating CD14 $^{+}$ monocytes between controls and patients with CAD. (F) Transfection with PIAS1 siRNA (siPIAS1) significantly facilitates the activated STAT1 luciferase activities induced by LPS (100 ng/mL) and IFN- γ (20 ng/mL) in HEK293T cells. ISRE indicates the Luciferase vectors containing STAT1 responsive elements. Each experiment was performed in triplicate. Data are presented as mean \pm SD. *, $P < 0.05$.

and circulating immune cells, plays an important role in controlling macrophage polarization and in atherosclerotic development (4,6). In accordance to our results, Sun *et al.* (25) revealed that circulating miR-181b in the plasma was markedly reduced in CAD patients and in apolipoprotein E-deficient mice with a high-fat diet. However, the endogenous causation leading to the decline in miR-181b expression in CAD patients remains unclear. Toward this end, we performed MethyLight PCR and pyrosequencing, finding the specific methylated CpG sites at the promoter of miR-181b in CAD patients. A growing

evidence of studies has uncovered alterations in DNA methylation at indicated promoters in specific cell types during the development of ASCVD (26). Among divergent types of circulating myeloid cells, monocytes are considered to play the most critical effect in the pathogenesis of atherosclerosis, because they are able to infiltrate into subendothelial, differentiate into pro-inflammatory M1 phenotype and anti-inflammatory M2 phenotype (5). Therefore, our findings propose that miR-181b hypermethylation in circulating monocytes may explain the decreased expression of miR-181b in CAD patients and

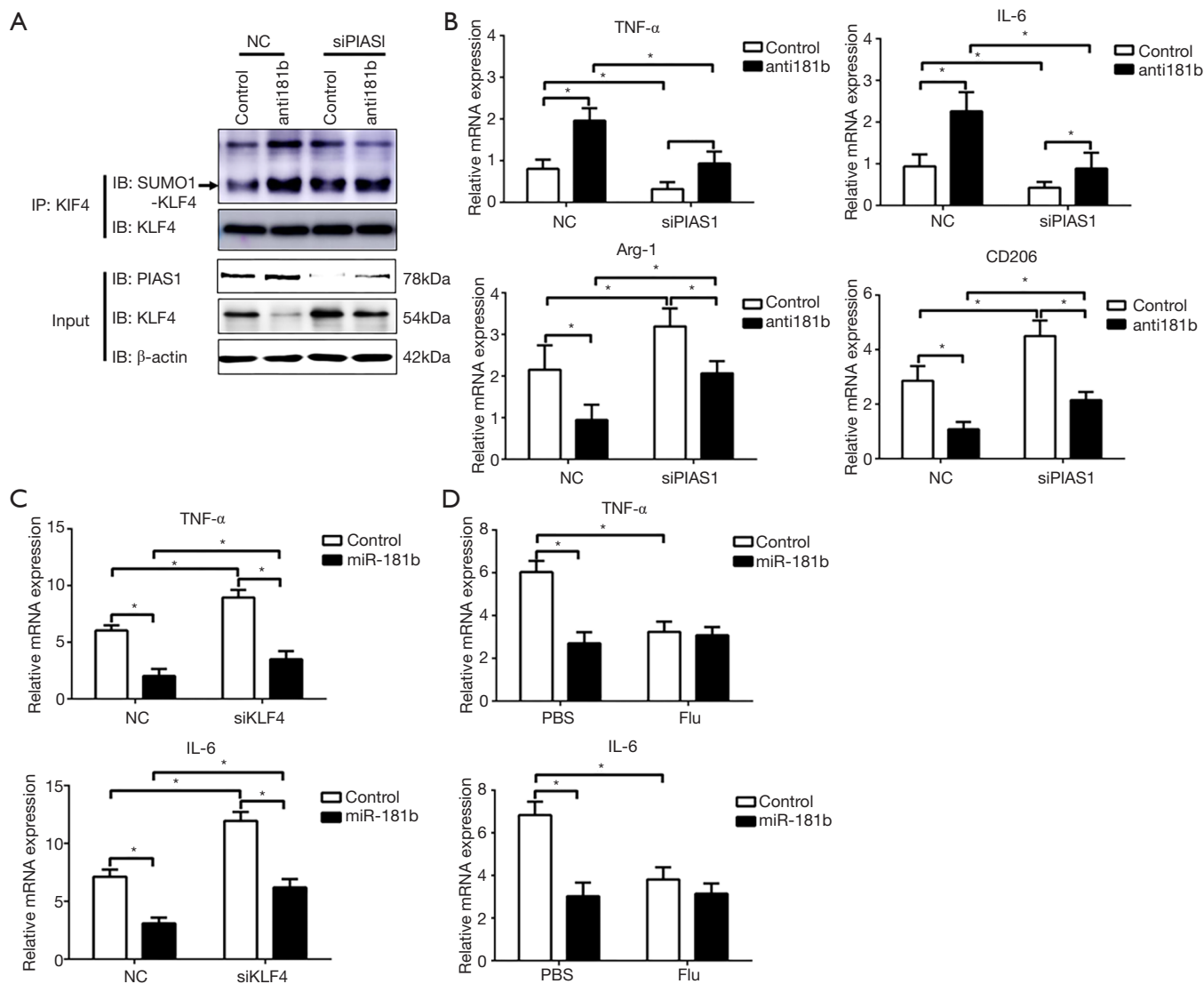


Figure 6 MiR-181b suppresses KLF4 SUMOylation and drives M2 polarization via interaction with PIAS1. (A) Endogenous SUMO1 conjugates of KLF4 are determined by co-immunoprecipitation in the lysates of macrophages co-transfected with miR-181b inhibitors and PIAS1 siRNA. (B) Quantification of M1 and M2 markers in macrophages co-transfected with miR-181b inhibitors (anti181b) and PIAS1 siRNA (siPIAS1). (C) Quantification of M1 markers in macrophages co-transfected with miR-181b mimics and KLF4 siRNA (siKLF4). (D) Quantification of M1 markers in macrophages transfected with miR-181b mimics in the presence of Fludarabine for 12 hours (Flu, 50 μ M). Each experiment was performed in triplicate. Data are presented as mean \pm SD. *, $P < 0.05$.

become a promising marker for ASCVD.

It has been previously reported that increases in M1 phenotype and decreases in M2 phenotype are accompanied with the progression of atherosclerosis (27). Similar to the previous report, miR-181b was induced by LPS treatment and highly expressed in M1 subsets (28). The previous study had identified C/EBP β as one of miR-181b target genes and confirmed that miR-181b inhibited M2 polarization

via suppression of C/EBP β (29). However, apart from C/EBP β , many other lineage-specifying transcription factors, e.g., KLF4, KLF6, YAP and STAT1, have been shown to cooperatively govern macrophage polarization. While the mRNA expression of these transcription factors remained unchanged, the protein expression of KLF4 was prominently increased by overexpression of miR-181b. KLF4 acts as a critical transcription factor and centrally integrates multiple

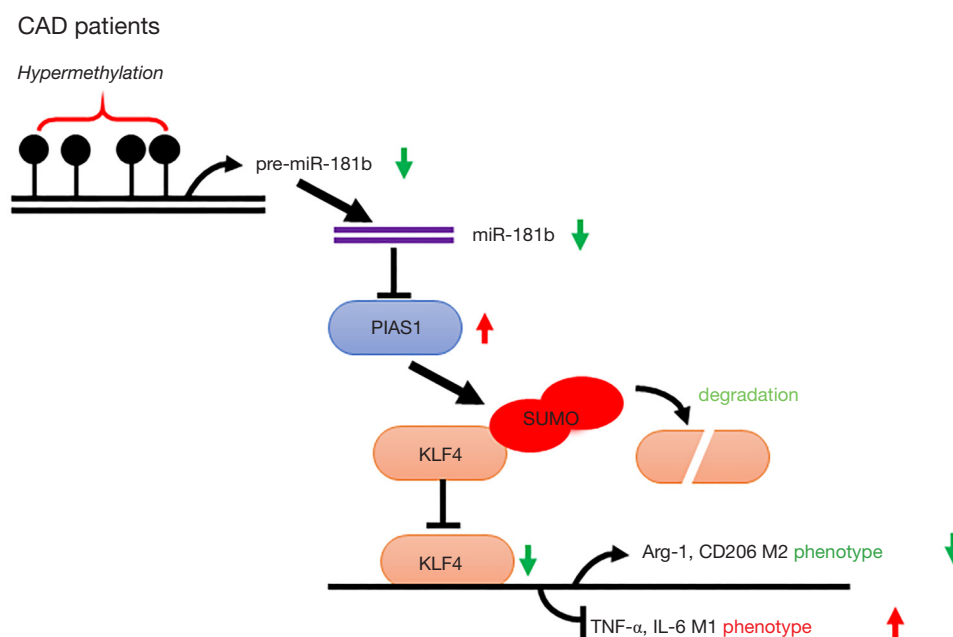


Figure 7 Schematic diagram of miR-181b hypermethylation in patients with coronary artery disease and miR-181b-PIAS1 axis in macrophage polarization. Hypermethylation of miR-181b promoter in circulating monocytes of patients with coronary artery disease (CAD) results in lower expression of miR-181b as compared with healthy individuals. Decreased miR-181b inhibits the expression of KLF4 via restoring PIAS1 and promoting KLF4 SUMOylation, eventually facilitating M1 polarization and alleviating M2 polarization.

signal inputs in the pathogenesis of atherosclerosis (30,31). Li *et al.* (9) provided strong evidences that KLF4 retarded atherosclerotic progression via synergistically alleviating inflammation in endothelial cells and facilitating M1 to M2 phenotypic transition. In line with these results, we further accentuate that increased KLF4 by overexpression of miR-181b lead up to M2 phenotypic switch. By contrast, Wang *et al.* (32) observed that SUMOylation of KLF4 coordinated macrophages to polarize into M2 phenotype via enhancing the binding of KLF4 to Arg-1 upon IL-4 stimulation. This seemingly contradictory results could be explained by the fact that IL-4-induced KLF4 SUMOylation augmented KLF4 transcription activity but did not alter its expression and stability.

Another critical question is how miR-181b indirectly changes the protein expression of KLF4 via post-transcriptional modification. In the present study, delivery of miR-181b disturbs the M1 polarity switch through induction of KLF4 SUMOylation and degradation. In this regard, we show that knockdown of miR-181b exerts a facilitating action on M1 polarity via targeting PIAS1. Of note, PIAS1 belongs to the largest group of SUMO E3 ligase characterized by a SP-RING motif and is considered

as the most critical one of E3 ligases (33). A number of researches has shown that PIAS1-linked SUMOylation of target transcription factor is engaged in diverse physiological progression and pathogenesis of numerous diseases (34,35). During the past two decades, several researchers have identified that the specific proteins were degraded by small ubiquitin-like modification (36). SUMOylation is referred to be a reversible procedure catalyzed by its own E1, E2 and E3 enzymes and is allowed to be restored by a diversity of SUMO-specific proteases (34,37). In line with the above observations, we demonstrated that knockdown of miR-181b augments KLF4 SUMOylation through promoting PIAS1 expression. Additionally, Kawai-Kowase *et al.* (38) delineated that PIAS1 induced KLF4 SUMOylation followed by proteasome degradation upon TGF- β stimulation in VSMCs. Given a direct modulation of miR-181b on PIAS1, it is likely that miR-181b has pleiotropic roles in the protein SUMOylation and in the pathogenesis of cardiovascular diseases.

Conclusions

Our data in clinical blood samples and molecular

experiments highlight miR-181b as an epigenetic marker for atherosclerotic development and uncover its role in KLF4 SUMOylation and macrophage polarization via directly targeting PIAS1.

Acknowledgments

Funding: None.

Footnote

Data Sharing Statement: Available at <http://dx.doi.org/10.21037/cdt-20-407>

Conflicts of Interest: All authors have completed the ICMJE uniform disclosure form (available at <http://dx.doi.org/10.21037/cdt-20-407>). The authors have no conflicts of interest to declare.

Ethical Statement: The authors are accountable for all aspects of the work in ensuring that questions related to the accuracy or integrity of any part of the work are appropriately investigated and resolved. The clinical trial was approved by the First Affiliated Hospital of Harbin Medical University Ethics Committee (Ethical approval ID: HMU-2018-124). The informed written consent was provided in accordance with the Declaration of Helsinki (as revised in 2013) and obtained from the whole enrollment.

Open Access Statement: This is an Open Access article distributed in accordance with the Creative Commons Attribution-NonCommercial-NoDerivs 4.0 International License (CC BY-NC-ND 4.0), which permits the non-commercial replication and distribution of the article with the strict proviso that no changes or edits are made and the original work is properly cited (including links to both the formal publication through the relevant DOI and the license). See: <https://creativecommons.org/licenses/by-nc-nd/4.0/>.

References

1. GBD 2016 Causes of Death Collaborators. Global, regional, and national age-sex specific mortality for 264 causes of death, 1980-2016: a systematic analysis for the Global Burden of Disease Study 2016. *Lancet* 2017;390:1151-210.
2. Tabas I, Lichtman AH. Monocyte-Macrophages and T Cells in Atherosclerosis. *Immunity* 2017;47:621-34.
3. Robbins CS, Hilgendorf I, Weber GF, et al. Local proliferation dominates lesional macrophage accumulation in atherosclerosis. *Nat Med* 2013;19:1166-72.
4. Groh L, Keating ST, Joosten LAB, et al. Monocyte and macrophage immunometabolism in atherosclerosis. *Semin Immunopathol* 2018;40:203-14.
5. Murray PJ. Macrophage Polarization. *Annu Rev Physiol* 2017;79:541-66.
6. Gordon S, Martinez FO. Alternative activation of macrophages: mechanism and functions. *Immunity* 2010;32:593-604.
7. Rougeot J, Torraca V, Zakrzewska A, et al. RNAseq Profiling of Leukocyte Populations in Zebrafish Larvae Reveals a cxcl11 Chemokine Gene as a Marker of Macrophage Polarization During Mycobacterial Infection. *Front Immunol* 2019;10:832.
8. Lv LL, Feng Y, Wu M, et al. Exosomal miRNA-19b-3p of tubular epithelial cells promotes M1 macrophage activation in kidney injury. *Cell Death Differ* 2020;27:210-26.
9. Li Z, Martin M, Zhang J, et al. Kruppel-Like Factor 4 Regulation of Cholesterol-25-Hydroxylase and Liver X Receptor Mitigates Atherosclerosis Susceptibility. *Circulation* 2017;136:1315-30.
10. Shankman LS, Gomez D, Cherepanova OA, et al. KLF4-dependent phenotypic modulation of smooth muscle cells has a key role in atherosclerotic plaque pathogenesis. *Nat Med* 2015;21:628-37.
11. Stavri S, Simionescu M, Kardassis D, et al. Kruppel-like factor 4 synergizes with CREB to increase the activity of apolipoprotein E gene promoter in macrophages. *Biochem Biophys Res Commun* 2015;468:66-72.
12. Essandoh K, Li Y, Huo J, et al. MiRNA-Mediated Macrophage Polarization and its Potential Role in the Regulation of Inflammatory Response. *Shock* 2016;46:122-31.
13. Canfran-Duque A, Rotllan N, Zhang X, et al. Macrophage deficiency of miR-21 promotes apoptosis, plaque necrosis, and vascular inflammation during atherogenesis. *EMBO Mol Med* 2017;9:1244-62.
14. Ganta VC, Choi MH, Kutateladze A, et al. A MicroRNA93-Interferon Regulatory Factor-9-Immuno-responsive Gene-1-Itaconic Acid Pathway Modulates M2-Like Macrophage Polarization to Revascularize Ischemic Muscle. *Circulation* 2017;135:2403-25.
15. Jiang D, Sun M, You L, et al. DNA methylation and hydroxymethylation are associated with the degree of

- coronary atherosclerosis in elderly patients with coronary heart disease. *Life Sci* 2019;224:241-8.
16. Zhong W, Li B, Xu Y, et al. Hypermethylation of the Micro-RNA 145 Promoter Is the Key Regulator for NLRP3 Inflammasome-Induced Activation and Plaque Formation. *JACC Basic Transl Sci* 2018;3:604-24.
 17. Kolossvary M, Szilveszter B, Edes IF, et al. Comparison of Quantity of Coronary Atherosclerotic Plaques Detected by Computed Tomography Versus Angiography. *Am J Cardiol* 2016;117:1863-7.
 18. Ferguson JF, Hinkle CC, Mehta NN, et al. Translational studies of lipoprotein-associated phospholipase A(2) in inflammation and atherosclerosis. *J Am Coll Cardiol* 2012;59:764-72.
 19. Zhuang J, Peng W, Li H, et al. Methylation of p15INK4b and expression of ANRIL on chromosome 9p21 are associated with coronary artery disease. *PLoS One* 2012;7:e47193.
 20. An Y, Chen XM, Yang Y, et al. LncRNA DLX6-AS1 promoted cancer cell proliferation and invasion by attenuating the endogenous function of miR-181b in pancreatic cancer. *Cancer Cell Int* 2018;18:143.
 21. Liu B, Liao J, Rao X, et al. Inhibition of Stat1-mediated gene activation by PIAS1. *Proc Natl Acad Sci U S A* 1998;95:10626-31.
 22. Zhang X, Yu J, Zhao C, et al. MiR-181b-5p modulates chemosensitivity of glioma cells to temozolomide by targeting Bcl-2. *Biomed Pharmacother* 2019;109:2192-202.
 23. Indrieri A, Carrella S, Romano A, et al. miR-181a/b downregulation exerts a protective action on mitochondrial disease models. *EMBO Mol Med* 2019;11:e8734.
 24. Pang X, Feng G, Shang W, et al. Inhibition of lncRNA MEG3 Protects Renal Tubular From Hypoxia-Induced Kidney Injury in Acute Renal Allografts by Regulating miR-181b/TNF- α Signaling Pathway. *J Cell Biochem* 2019;120:12822-31.
 25. Sun X, He S, Wara AKM, et al. Systemic delivery of microRNA-181b inhibits nuclear factor-kappaB activation, vascular inflammation, and atherosclerosis in apolipoprotein E-deficient mice. *Circ Res* 2014;114:32-40.
 26. Duan L, Hu J, Xiong X, et al. The role of DNA methylation in coronary artery disease. *Gene* 2018;646:91-7.
 27. Shapouri-Moghaddam A, Mohammadian S, Vazini H, et al. Macrophage plasticity, polarization, and function in health and disease. *J Cell Physiol* 2018;233:6425-40.
 28. Zhang W, Shen X, Xie L, et al. MicroRNA-181b regulates endotoxin tolerance by targeting IL-6 in macrophage RAW264.7 cells. *J Inflamm (Lond)* 2015;12:18.
 29. Su R, Lin HS, Zhang XH, et al. MiR-181 family: regulators of myeloid differentiation and acute myeloid leukemia as well as potential therapeutic targets. *Oncogene* 2015;34:3226-39.
 30. Han YH, Kim HJ, Na H, et al. RORalpha Induces KLF4-Mediated M2 Polarization in the Liver Macrophages that Protect against Nonalcoholic Steatohepatitis. *Cell Rep* 2017;20:124-35.
 31. He M, Huang TS, Li S, et al. Atheroprotective Flow Upregulates ITPR3 (Inositol 1,4,5-Trisphosphate Receptor 3) in Vascular Endothelium via KLF4 (Kruppel-Like Factor 4)-Mediated Histone Modifications. *Arterioscler Thromb Vasc Biol* 2019;39:902-14.
 32. Wang K, Zhou W, Cai Q, et al. SUMOylation of KLF4 promotes IL-4 induced macrophage M2 polarization. *Cell Cycle* 2017;16:374-81.
 33. Rott R, Szargel R, Shani V, et al. SUMOylation and ubiquitination reciprocally regulate alpha-synuclein degradation and pathological aggregation. *Proc Natl Acad Sci U S A* 2017;114:13176-81.
 34. Jones MC, Fusi L, Higham JH, et al. Regulation of the SUMO pathway sensitizes differentiating human endometrial stromal cells to progesterone. *Proc Natl Acad Sci U S A* 2006;103:16272-7.
 35. Roukens MG, Alloul-Ramdhani M, Versteeg AC, et al. Identification of a new site of sumoylation on Tel (ETV6) uncovers a PIAS-dependent mode of regulating Tel function. *Mol Cell Biol* 2008;28:2342-57.
 36. Chang SC, Ding JL. Ubiquitination and SUMOylation in the chronic inflammatory tumor microenvironment. *Biochim Biophys Acta Rev Cancer* 2018;1870:165-75.
 37. Gong L, Qi R, Li DW. Sumoylation Pathway as Potential Therapeutic Targets in Cancer. *Curr Mol Med* 2017;16:900-5.
 38. Kawai-Kowase K, Ohshima T, Matsui H, et al. PIAS1 mediates TGFbeta-induced SM alpha-actin gene expression through inhibition of KLF4 function-expression by protein sumoylation. *Arterioscler Thromb Vasc Biol* 2009;29:99-106.

Cite this article as: Wang Z, Li C, Sun X, Li Z, Li J, Wang L, Sun Y. Hypermethylation of miR-181b in monocytes is associated with coronary artery disease and promotes M1 polarized phenotype via PIAS1-KLF4 axis. *Cardiovasc Diagn Ther* 2020;10(4):738-751. doi: 10.21037/cdt-20-407

Supplementary

Table S1 Summary of quantitative RT-PCR and MethyLight primer and probe sequences

Gene (Ref.)	Primer (5'→3')	Probe
MethyLight		
<i>MiR-181b</i>	Forward: 5'-GGA ATG TAA GAG TAT TTA TTA GCG G-3' Reverse: 5'-ACC CCA AAA TAC AAT CAA CGA T-3'	
<i>ACTB</i>	Forward: 5'-TGG TGA TGG AGG AGG TTT AGT AAG T-3' Reverse: 5'-AAC CAA TAA AAC CTA CTC CTC CCT TAA-3'	6FAM-ACCACCACCCAACACACAATAACAAACACA-BHQ1
Pyrosequencing		
<i>MiR-181b</i>	Forward: 5'-GAT TTG AAA TTT AGA GAG GAA TGT AAG AG-3' Reverse: 5'-ATA AAA ACC CCA AAA TAC AAT CAA C-3'	5'-ATTTGAAATTTAGAGAGGAATGTAAGAGTA-3'
<i>MiR-181b-LUC-KpnI</i>	Forward: 5'-GGT ACC GTA AGA GCA TCC ATC Reverse: 5'-GGT ACC GTA CAG TCA ACG GTC AGT G	
Quantitative PCR		
<i>TNF-α</i>	Forward: 5'-CCT CTC TCT AAT CAG CCC TCT G-3' Reverse: 5'-GAG GAC CTG GGA GTA GAT GAG-3'	
<i>IL-6</i>	Forward: 5'-ACT CAC CTC TTC AGA ACG AAT TG-3' Reverse: 5'-CCA TCT TTG GAA GGT TCA GGT TG-3'	
<i>Arg-1</i>	Forward: 5'-GTG GAA ACT TGC ATG GAC AAC-3' Reverse: 5'-AAT CCT GGC ACA TCG GGA ATC-3'	
<i>CD206</i>	Forward: 5'-TCC GGG TGC TGT TCT CCT A-3' Reverse: 5'-CCA GTC TGT TTT TGA TGG CAC T-3'	
<i>GADPH</i>	Forward: 5'-GGA GCG AGA TCC CTC CAA AAT-3' Reverse: 5'-GGC TGT TGT CAT ACT TCT CAT GG-3'	